6

Effect of Bioactive Growth Surfaces on Human Mesenchymal Stem Cells: A Pilot Biomarker Study to Assess Growth and Differentiation

Liliana Craciun[1], Pranela Rameshwar[2], Steven J. Greco[2], Ted Deisenroth[1] and Carmen Hendricks-Guy[1]

[1]BASF Corporation, 500 White Plains Road, Tarrytown, NY 10591, USA
[2]New Jersey Medical School, Department of Medicine – Division of Hematology/Oncology, Rutgers School of Biomedical Health Science, Newark, NJ 07103, USA

Abstract

Mesenchymal stem cells (MSCs) are multipotent adult stem cells with the ability to differentiate into multiple cell lineages, and possess significant potential towards application in cell therapy and tissue engineering. A significant barrier to the effective implementation of human MSC (hMSC) therapies is the limited access to large quantities of viable, homogeneous cell populations produced in reproducible, consistent cultures. hMSCs are adherent cells whose morphology, as well as proliferation and differentiation potential, depend on the characteristics of the tissue culture surface they grow on. In the present study, we screened a panel of plastic surfaces possessing various physical characteristics for their ability to expand and maintain hMSCs in an undifferentiated state. The purpose of these studies was to identify materials which outperform conventional tissue culture polystyrene (TCPS). The plastic surfaces that were investigated were created by injection molding and were used either "as is" or after plasma treatment under an oxidative or reductive atmosphere. After 5 days culture, the effect of the growth surfaces on stem cell maintenance and differentiation was quantified by the expression of stem cell markers (OCT-4; NANOG; NOTCH1; PH-4; p21).

Several surfaces exhibited an increase in the stem cell specific- and/or a decrease in the differentiation-specific genes, indicating a "positive result" compared to the TCPS reference standard. Of the many surface physical characteristics, the roughness and fibrous structure of a glass fiber-reinforced poly(styrene-acrylonitrile) polymeric surface had the most prevalent effect on facilitating hMSC expansion with preservation of stem cell function. These findings are not only significant in defining ideal conditions for hMSC growth in culture, but have broader implications for tissue engineering.

Keywords: Human Mesenchymal Stem Cells, Bioactive surface, Cell growth, Cell differentiation.

6.1 Introduction

Cell therapies show great promise for repairing or regenerating damaged cells, tissues and organs. Cells can carry out functions that cannot be performed by small-molecule drugs. They are adaptable and can sense their surroundings and vary their responses to better suit physiologic conditions. In particular, stem cells have both the long term capacity to replicate themselves, thereby maintaining a continuous cell supply, as well as the ability to differentiate into specialized cell types. By leveraging the capacity for self-renewal and regeneration, stem cell therapies, also referred to as regenerative or reparative medicine, offer hope for solving critical, unmet needs for a multitude of diseases and disorders, many of which are currently untreatable.

The therapeutic use of stem cells has been ongoing for several decades in the form of bone marrow (BM) transplants to treat various hematological disorders and immune-related diseases, and is a very active area of investigation [1–6]. In mammals there are two broad types of stem cells, embryonic stem cells (ESC) and non-embryonic or "adult" stem cells. The primary role of adult stem cells in living organisms is to maintain and repair the tissue in which they are found. Mesenchymal stem cells (MSC) are multi-potent adult stem cells available in bone marrow and adipose tissue [7–9]. They can differentiate into cell types such as adipocytes, osteoblasts, chondrocytes, cardiomyocytes, or neuronal cells, supporting the formation of blood and fibrous connective tissue [10–13]. MSC represent an ideal source for cellular replacement therapies because of their relative ease of isolation, high *in vitro* expansion rate, and demonstrated multipotency. In addition, MSCs suppress immune system rejection in individuals receiving them, increasing the likelihood of treatment success [14–22]. These properties circumvent host immune response issues

allowing allogeneic cell sources which could be immediately available as an off-the-shelf therapy. Another advantage of MSCs is a lower probability of tumor formation compared to ESCs [4, 23, 24].

There is great interest in applications of MSCs in cell therapy and tissue engineering. MSCs are being tested for a variety of disorders with more than 360 active clinical trials in the US alone, where MSCs are evaluated in diseases including graft-versus-host disease, Crohn's disease, myocardial infarction, colitis, diabetes, cartilage defects, bone cysts, limb ischemia, Parkinson, arthritis, anemia, stroke, nephropathy, and many others. The first MSC drug therapy was approved by Canada in 2012 to treat children in graft vs. host disease, a nearly fatal complication arising during bone marrow transplantation.

However, using MSCs for medical treatments still poses problems that affect their clinical usefulness. Major challenges include the need to ensure safety, efficacy, consistent performance, and the ability to produce large quantities of homogeneous cell populations needed for clinical applications and treatment. MSCs must be amplified in culture by repeated passaging to create enough viable cells, however, prolonged expansion could potentially reduce the ability of the cells to differentiate. In cell-based therapies, cells are removed from the patient or a healthy donor and cultured in the laboratory where they are expanded before being infused into the patient. Cells expanded outside of their natural environment in the human body can become ineffective or produce adverse effects. MSCs are adherent cells whose cell morphology, proliferation and differentiation potential are affected by the surface they are grown on. To this end, the purpose of the present study was to investigate synthetic materials suitable for either supporting the growth and maintenance of MSCs in undifferentiated state or facilitating stem cell differentiation into specialized tissues. Herein, we screened a panel of plastic surfaces with different physical characteristics in order to identify materials which outperform conventional tissue culture polystyrene (TCPS). The plastic surfaces were created by injection molding and were used either "as is" or after plasma treatment under an oxidative or reductive atmosphere. Several surfaces exhibited a statistically significant increase in the stem cell specific-genes and/or a decrease in the differentiation-specific genes, indicating a "positive result" compared to the TCPS reference standard. Of the many surface physical characteristics the roughness and fibrous structure of a glass fiber-reinforced poly(styrene-acrylonitrile) polymeric surface had the most prevalent effect on facilitating hMSC expansion with preservation of stem cell function.

6.2 Materials and Methods

6.2.1 Materials

The polymer materials were sourced from BASF (Ultraform N 2320 003 Q600, Ultrason S 2010, UltraPET PCS Clear, Ultramid B27 E, Terluran GP-22, Terlux 2802, Terlux 2812, Styrolux 656 C, Styrolux 3G 46, Luran 378 P, Luran 378 PG-7) and Topas Advanced Polymers (Topas 6013S-04). Polymer chemistries and abbreviations are shown in Table 6.1.

Polymer processing was done by injection molding into 1 mm thick plaques using 170-tons Van Dorn (POM, PSU, PET, PA6) and Boy 50 M (ABD, MABS, SBC, SAN, COC) horizontal injection molding machines (BASF Engineering Plastics; Budd Lake and Tarrytown Laboratories). The polymer plaques had either a matte (rough) or a glossy (smooth) finish. They were cut into round coverslips of 35 mm diameter that fit into 6-well plates for cell culture. In addition the coverslips were chemically modified by plasma treatment. All samples were carefully cleaned from contaminants by washing with organic solvents and water in an ultrasonic bath. During plasma treatment the coverslips were exposed to atmospheric chemical plasmas of different compositions at 25 WD (500 W@11 fpm) using Enercon Tangential Plasma3 technology with a 1 mm electrodes air gap (Enercon Industries, Menomonee Falls, WI). The treatment conditions were: (a) 90% (90% N_2 + 10% H_2) + 10% O_2; (b) 90% N_2 + 10% NH_3; and (c) 80% helium + 20% O_2. It is expected that the reductive conditions (a & b) would increase the nitrogen content at

Table 6.1 Materials utilized in study

Abbreviation	Chemical Name	Trade Name
POM	Poly(oxymethylene)	Ultraform N 2320 003 Q600
PSU	Polysulfone	Ultrason S 2010
PET	Poly(ethylene terephthalate)	UltraPet PCS Clear
PA6	Polyamide 6; poly(ε-caprolactam); nylon 6	Ultramid B27 E
ABS	Poly(acrylonitrile-1,3-butadiene-styrene)	Terluran GP-22
MABS	Poly(methyl methacrylate-acrylonitrile-1,3-butadiene-styrene)	Terlux 2802; Terlux 2812
SBC	Polystyrene-*bloc*k-poly(1,3-butadiene)	Styrolux 656 C; Styrolux 3G 46
SAN	Poly(styrene-acrylonitrile)	Luran 378 P; Luran 378 PG-7
COC	Cyclo olefinic co-polymer; polyethylene-*bloc*k-polynorbornene	Topas 6013S-04

the surface, whereas the oxidative plasma (c) would oxidize the surface and potentially make it rougher.

The characterization of the polymeric surfaces before and after plasma treatment was done by contact angle with water, atomic force microscopy (AFM), and X-ray photoelectron spectroscopy (XPS). AFM analysis was performed with a Dimension V scanning probe microscope from Vecco, used in tapping mode with a Bruker TESP tip. Contact angle analysis was performed on an OCA 20 goniometer from Future Digital Scientific Corporation. XPS analysis was done with a K-Alpha X-ray Photoelectron Spectrometer from Thermal Fisher. Samples were mounted on a standard sample holder using clips to hold the materials in place. An X-ray spot size of 400 μm was analyzed using an ion gun current of 3000 eV with a sputter rate of 0.23 nm/sec.

The bulk elemental analysis for carbon, hydrogen and nitrogen was done by combustion followed by microchemical techniques. The % oxygen is calculated as the difference to 100%. The values reported are averages of duplicate runs. CHN Analysis is a form of Elemental Analysis concerned with determination of only Carbon (C), Hydrogen (H) and Nitrogen (N) in a sample. The most popular technology behind the CHN analysis is combustion train analysis where the sample is first fully combusted and then the products of its combustion are analyzed. The full combustion is usually achieved by providing abundant oxygen supply during the combustion process. The analyzed products, Carbon, Hydrogen and Nitrogen, oxidize and form carbon dioxide (CO_2), water, and nitric oxide (NO), respectively. These product compounds are carefully measured. The gases in individual traps for CO_2 and water are measured for thermal conductivity before and after combustion. The concentrations are used to determine the elemental composition, or *empirical formula*, of the analyzed sample.

6.2.2 Cell Culture Reagents

Dulbecco's modified Eagle's medium (DMEM) with high glucose, trypsin-EDTA and α-MEM was purchased from Gibco (Grand Island, NY), and fetal calf serum (FCS) from Hyclone Laboratories (Logan, UT).

6.2.3 Culture of Human MSCs

MSCs were cultured from BM aspirates as described [14]. The use of human BM aspirates followed a protocol approved by the Institutional Review

Board of The University of Medicine and Dentistry of New Jersey-Newark campus. Unfractionated BM aspirates (2 ml) were diluted in 12 ml of DMEM containing 10% FCS (D10 media) and then transferred to vacuum-gas plasma treated, tissue culture Falcon 3003 petri dishes. Plates were incubated, and at day 3, mononuclear cells were isolated by Ficoll Hypaque density gradient and then replaced in the culture plates. Fifty percent of media was replaced with fresh D10 media at weekly intervals until the adherent cells were approximately 80% confluent. After four cell passages, the adherent cells were asymmetric, $CD14^-$, $CD29^+$, $CD44^+$, $CD34^-$, $CD45^-$, $SH2^+$, prolyl-4-hydroxylase$^-$ [14].

6.2.4 qPCR for Stem Cell Markers

Test surfaces were divided into three experimental groups which were analyzed independently. Tissue-culture treated polystyrene (BD Falcon) and BD PureCoat amine multi-well plates from BD Biosciences were used as references. Sterilization was done by UV-exposure before cell seeding. MSC were cultured from bone marrow aspirates of healthy donors, aged 20–35. After 5 days of culture, cells were harvested from each surface using enzymatic detachment and pelleted by centrifugation. Total RNA (2 μg) was reverse transcribed, and 200 ng of cDNA was used in quantitative PCR (qPCR) with the Platinum SYBR Green qPCR SuperMix-UDG Kit (Invitrogen, Carlsbad, CA). qPCRs were normalized by amplifying the same sample of cDNA with primers specific for β-actin. qPCRs were performed with a 7500 Real Time PCR System (Applied Biosystems, Foster City, CA). The cycling profile for real-time PCR (40 cycles) was as follows: 94°C for 15 seconds and 60°C for 45 seconds. Gene expression analysis was performed using the 7500 System SDS software (Applied Biosystems). Normalizations were performed with β-actin, and values were arbitrarily assigned a value of 1. Primer sequences and additional information are as follows: **OCT4** (NM_002701, +789/+1136) Forward: gtt cag cca aaa gac cat, Reverse: cgt tgt gca tag cca ctg; **SOX2** (NM_003106, +734/+1113) Forward: aag gag cac ccg gat tat, Reverse: tgc gag tag gac atg ctg; **NANOG** (NM_024865, +686/1016) Forward: act ggc cga aga ata gca, Reverse: aaa gca gcc tcc aag tca; **PH-4** (NM_177939, +810/+1166) Forward: aag agt gtc ggc tca tca, Reverse: cac cag ctc act gga ctc; **p21** (NM_000389, +904/+1324) Forward: gcc agc tac ttc ctc ctc, Reverse: aag agg gaa aag gct caa; **β-Actin** (NM_001101, +842/+1037) Forward: tgc cct gag gca ctc ttc, Reverse: gtg cca ggg cag tga tct.

6.3 Results

Polymeric coverslips were made by injection molding with either a matte (M1 or M2) or a glossy (G) finish and treated with high density discharge atmospheric plasma using mixtures of air (nitrogen, oxygen) with an inert gas (helium) or other reactive gases (hydrogen, ammonia) for surface functionalization (Figure 6.1). The coverslips were run in an Enercon Plasma3 system above the lower electrode connected to the ground (Table 6.2). The air gap between the electrodes is occupied by the glowing reactive gases. Three different gaseous mixtures were used: a) 90% (90% N_2 + 10% H_2) + 10% O_2; (b) 90% N_2 + 10% NH_3; and (c) 80% helium + 20% O_2. The resulting plasma interacts with the surface inducing chemical and physical modifications. The effect of plasma on a given material is determined by the chemistry of the reactions between the surface and the reactive species present in the plasma. Each gas produces a unique plasma composition and results in different surface properties. Oxidative conditions (a & c) are known to result in formation of hydroxyl, aldehyde, ketone, and carboxyl groups at the surface [25]. Plasma treatment with ammonia gas (b) gives mainly amine-containing surfaces [26, 27]. The chemistry changes at the surface of the plasma treated coverslips were analyzed with XPS. The elemental analysis XPS data is shown in Tables 6.3 and 6.4.

The treated surfaces were characterized by contact angle with water before and immediately after plasma treatment. The contact angles for all surfaces decreased significantly after plasma treatment relative to the untreated surfaces. The values are recorded in Table 6.2. In addition, the surface aging effects upon storage were evaluated by contact angle measurements two months after the plasma treatment. All surfaces had their contact angle increase to almost the initial value before treatment (Figure 6.2).

The matte and glossy surfaces had significantly different roughness. AFM was used to determine the mean surface roughness (RMS). The plasma treatments did not change the surface topography or roughness except for the POM and PA6 materials. The RMS values are also recorded in Table 6.2.

Overall, after injection molding and plasma treatment, the nine commercial polymers created 80 distinct surfaces, of which 60 unique combinations were tested for MSC growth (15 distinct polymers with glossy and mate surface finishes, and 3 different plasma treatments). BD TCPS Falcon and BD PureCoat Amine plates served as reference standards. The polymeric surfaces were first screened for their ability to maintain stem cell gene expression through the use of the stem cell markers: OCT-4, NOTCH1 and NANOG (Figure 6.3).

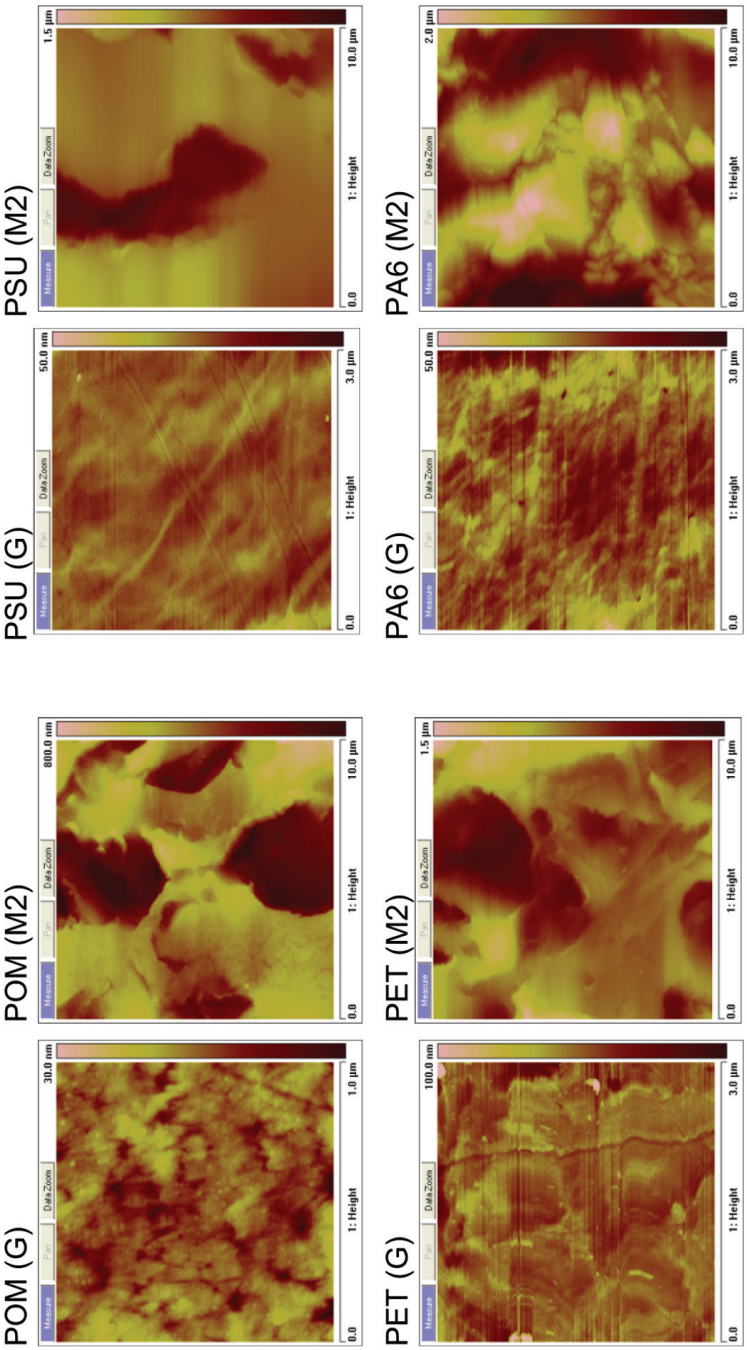

Figure 6.1 AFM phase images of plastic coverslips. AFM analysis was performed with a Dimension V scanning probe microscope from Vecco, used in tapping mode with a Bruker TESP vibrating cantilever tip. Sample height data is obtained from the changes in Z-axis displacement. The phase difference between the measured signal and the drive signal, caused by interactions between probe and material, gives the phase image, indicating regions of different composition and/or phase in the material.

Table 6.2 Characterization of plastic coverslips

No.	Surface	Modulus/Thermal	Surface Roughness[a]	Contact Angle[b] Initial	Contact Angle[b] at 2 Months
1.	**POM** (G)	2.7 GPa; no T_g; T_m 168°C	NT: RMS = 3 nm	NT:82	76
				a:43	80
				b:48	68
				c:42	68
2.	**POM** (M1)	2.7 GPa; no T_g; T_m 168°C	NT: RMS = 171 nm	NT:74	75
				a:48	73
				b:56	72
			RMS = 262 nm	c:54	74
3.	**POM** (M2)	2.7 GPa; no T_g; T_m 168°C	NT: RMS = 244 nm	NT:70	70
				a:47	68
				b:50	74
				c:47	69
4.	**PSU** (G)	2.6 GPa; T_g 190°C	NT: RMS = 5 nm	NT:79	80
				a:30	56
				b:46	70
				c:34	84
5.	**PSU** (M1)	2.6 GPa; T_g 190°C	NT: RMS = 70 nm	NT:66	79
				a:39	68
				b:47	64
				c:47	70
6.	**PSU** (M2)	2.6 GPa; T_g 190°C	NT: RMS = 167 nm	NT:72	87
				a:34	75
				b:39	68
				c:49	73
7.	**PET** (G)	3.5 GPa; T_g 82°C	NT: RMS = 7 nm	NT:87	72
				a:47	60
				b:38	68
				c:37	73
8.	**PET** (M1)	3.5 GPa; T_g 82°C	NT: RMS = 194 nm	NT:80	81
				a:34	63
				b:45	83
			RMS = 177 nm	c:47	57
9.	**PET** (M2)	3.5 GPa; T_g 82°C	NT: RMS = 211 nm	NT:78	76
				a:44	64
				b:38	63
				c:40	68
10.	**PA6** (G)	1 GPa; no T_g; T_m 221°C	NT: RMS = 5 nm	NT:66	66
				a:30	72
				b:39	71
				c:38	61
11.	**PA6** (M1)	1 GPa; no T_g; T_m 221°C	NT: RMS = 339 nm	NT:80	79
				a:38	80
			RMS = 604 nm	b:49	76
				c:51	72
12	**PA6** (M2)	1 GPa; no T_g; T_m 221°C	NT: RMS = 434 nm	NT:78	77
				a:44	66
				b:48	71
				c:50	80

(*Continued*)

Table 6.2 Continued

No.	Surface	Modulus/Thermal	Surface Roughness[a]	Contact Angle[b] Initial	at 2 Months
13.	**ABS** (G)	2.3 GPa; T_g 109°C	NT: RMS = 56 nm	NT:74	84
				a:48	71
				b:50	60
				c:44	70
14.	**MABS 2802** (G)	2 GPa; 109°C	NT: RMS = 17 nm	NT:68	73
				a:50	68
				b:48	71
				c:52	71
15.	**MABS 2812** (G)	1.9 GPa; T_g 104°C	NT: RMS = 18 nm	NT:83	71
				a:48	73
				b:44	66
				c:55	71
16.	**SBC 656 C** (G)	1.8 GPa; T_g 105°C	NT: RMS = 5 nm	NT:84	85
				a:34	78
				b:42	81
			RMS = 3nm	c:29	75
17.	**SBC 3G 46** (G)	1.64 GPa; no T_g	NT: RMS = 8 nm	NT:80	94
				a:38	81
				b:41	79
				c:47	82
18.	**SAN 378 P** (G)	3.8 GPa; T_g 110°C	NT: RMS = 7 nm	NT:83	74
				a:35	68
				b:42	55
				c:34	62
19.	**SAN 378 PG-7** (G)	12 GPa; T_g 113°C	NT: RMS = 235 nm	NT:85	82
				a:33	58
				b:39	48
			RMS = 232 nm	c:35	61
20.	**COC** (G)	COC	NT: RMS = 11 nm	NT:90	91
		2.9 GPa; T_g 139°C		a:43	79
				b:46	64
				c:34	79
21.	**TCPS**	3–3.5 GPa	RMS = 4 nm		
		T_g 100°C			
22.	**BD PureCoat Amine**	coated PS	RMS = 4 nm	NT:77	

[a]nd = not yet determined. NT = not treated or "as is". RMS = surface roughness. [b]Contact angle of water. Treatment conditions: (a) 90% (90% N_2 + 10% H_2) + 10% O_2; (b) 90% N_2 + 10% NH_3; and (c) 80% helium + 20% O_2.

After 5 days of culture, MSCs displayed an increase in the stem cell-specific markers compared to reference for a number of the initial surfaces tested. This result led us to investigate whether similar effects were observed with the remainder of the surfaces created. Again, we assessed stem cell-specific markers (Figure 6.4a) as well as markers of differentiation (p21, PH4) (Figure 6.4b). For surfaces that were able to be imaged by light microscopy,

Table 6.3 XPS and bulk elemental analysis of plastic coverslips

Sample/Element	C [wt %]	H [wt %]	N [wt %]	O [wt %]	Ratio O/C
MABS 2802					
Bulk elemental analysis	78.4	8.7	1.9	11.0	0.14
G-a	79.1		2.0	17.0	0.21
G-b	75.3		4.0	18.4	0.24
G-c	79.8		2.4	17.1	0.21
ABS GP-22					
Bulk elemental analysis	86.6	8.2	5.3	0	0
G-NT	91.3		4.0	4.7	0.05
G-b	81.6		7.0	10.5	0.13
G-c	84.7		4.7	10.3	0.13
POM					
Calculated elemental analysis	40.0	6.7	0	53.3	1.33
M1-a	52.6		0.7	42.1	0.80
M1-c	51.0		1.2	44.7	0.88
SAN 378 P					
Bulk elemental analysis	84.4	7.2	8.5	0	0
G-a	75.1		5.2	15.0	0.20
G-b	78.4		7.3	12.1	0.15
G-c	81.2		6.1	11.1	0.14
SBC 656 C					
G-NT	97.4		0.9	1.6	0.02
G-a	80.3		1.1	15.2	0.19
G-b	77.5		3.5	14.2	0.18
G-c	68.3		0.8	22.7	0.33
BD PureCoat Amine	79.6		6.5	12.7	0.16

Table 6.4 XPS data analysis of SBC 656 C coverslips

Sample/Element ID[a,b]	SBC 656 C	SBC 656 C	SBC 656 C	SBC 656 C
Element/ID[1]	G-NT	G-a	G-b	G-c
C CH_x	89.2	53.0	68.3	57.1
C CO	4.4	16.5	5.2	2.6
C CO_2 + CO_3	1.0	2.4	3.3	7.6
C aromatic, C(halide)	2.6	1.0	0.7	1.0
N nitride, NH_3	1.0	1.0	3.5	0.8
N NO, NH_4	nd	0.6	nd	nd
O	1.8	20.5	14.2	22.7

[a]Chemical state identifications are based on consistencies between reference and measured binding energies and are not absolute. [b] nd = not detected.

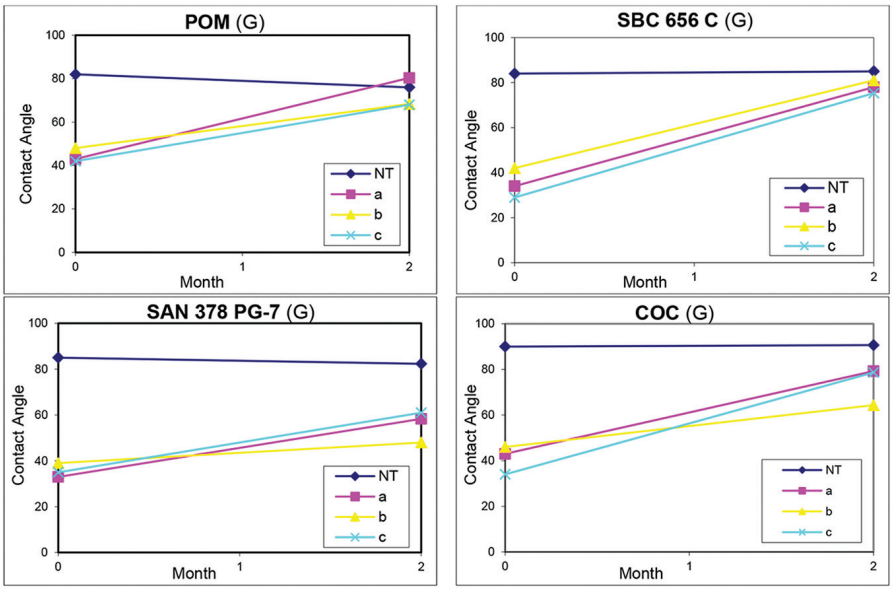

Figure 6.2 Water contact angle of POM, SBC 656 C, SAN 378 PG-7, and COC coverslips immediately after (month = 0) and two months (month = 2) after plasma treatment. The analysis was performed on an OCA 20 goniometer from Future Digital Scientific Corporation, by the sessile drop method. The optical system captures the profile of the water droplet on the surface. The angle between the water/solid interface is the contact angle. A low contact angle with water means that the surface is hydrophilic. A surface with a high water contact angle, usually larger than 90°, is considered hydrophobic.

cell morphologies were additionally examined (Figure 6.5). From the 60 different surfaces evaluated, 12 performed significantly better than the polystyrene reference surface in up-regulating stem-cell specific and down-regulating differentiation-specific genes. Future studies are necessary to validate whether these test surfaces can also maintain long-term stem cell expansion, to discern any global changes in stem cell gene expression through microarray analyses and to confirm that functionality is maintained through examining lineage-specific differentiation.

6.4 Discussion

The scope of this work was to evaluate the ability of standard polymeric materials to serve as tissue-culture surfaces for expansion and maintenance of stem cell phenotype in hMSCs. Plasma-treated polystyrene (TCPS) is

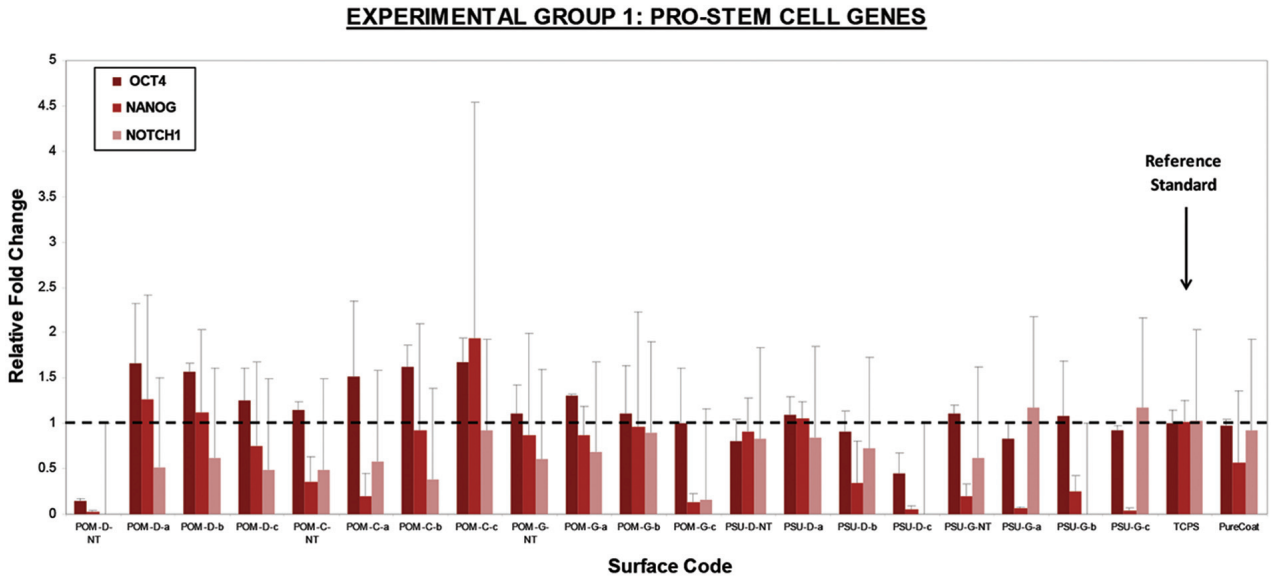

Figure 6.3 Effect of plastic surfaces on relative pro-stem cell gene expression in MSC cultures. After 5 days of culture, cells were harvested and RNA analyzed by qPCR for the stem cell genes, OCT4, NOTCH1 and NANOG. Normalizations were performed with β-actin, and values were arbitrarily assigned a value of 1 relative to BD TCPS Falcon. BD PureCoat Amine plates also served as a reference material.

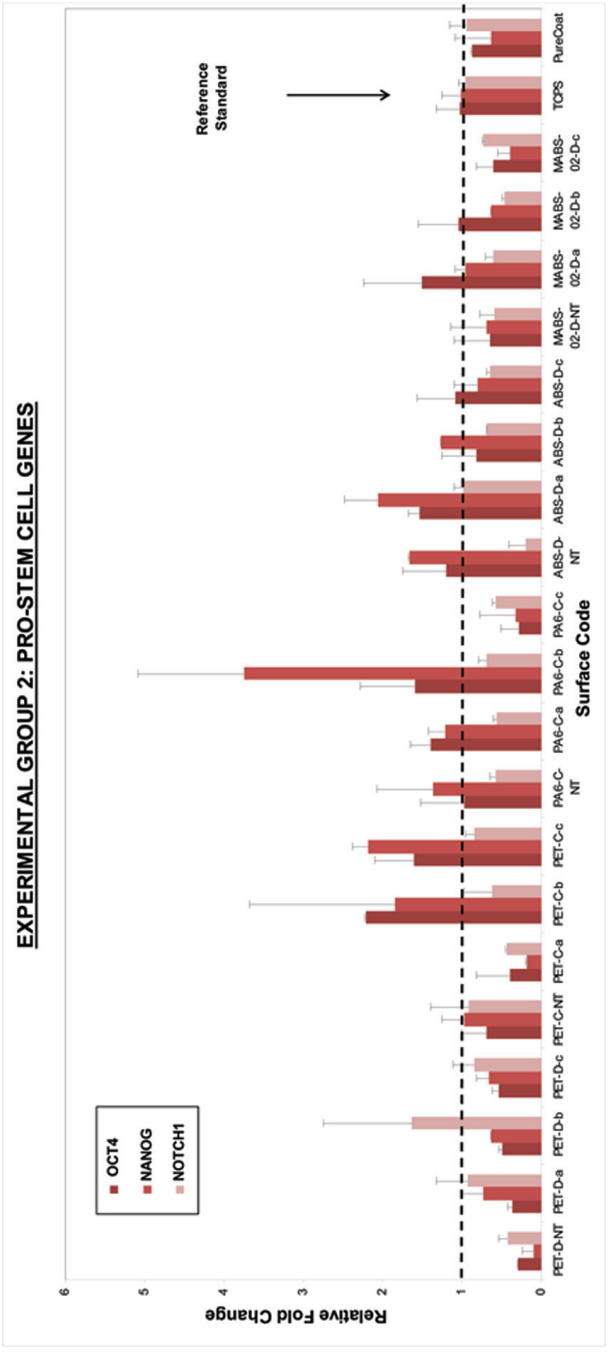
EXPERIMENTAL GROUP 2: PRO-STEM CELL GENES
OCT4
NANOG
NOTCH1
Reference Standard
Relative Fold Change
0
1
2
3
4
5
6
PET-D-NT
PET-D-a
PET-D-b
PET-D-c
PET-C-NT
PET-C-a
PET-C-b
PET-C-c
PA6-C-NT
PA6-C-a
PA6-C-b
PA6-C-c
ABS-D-NT
ABS-D-a
ABS-D-b
ABS-D-c
MABS-02-D-NT
MABS-02-D-a
MABS-02-D-b
MABS-02-D-c
TCPS
PureCoat
Surface Code

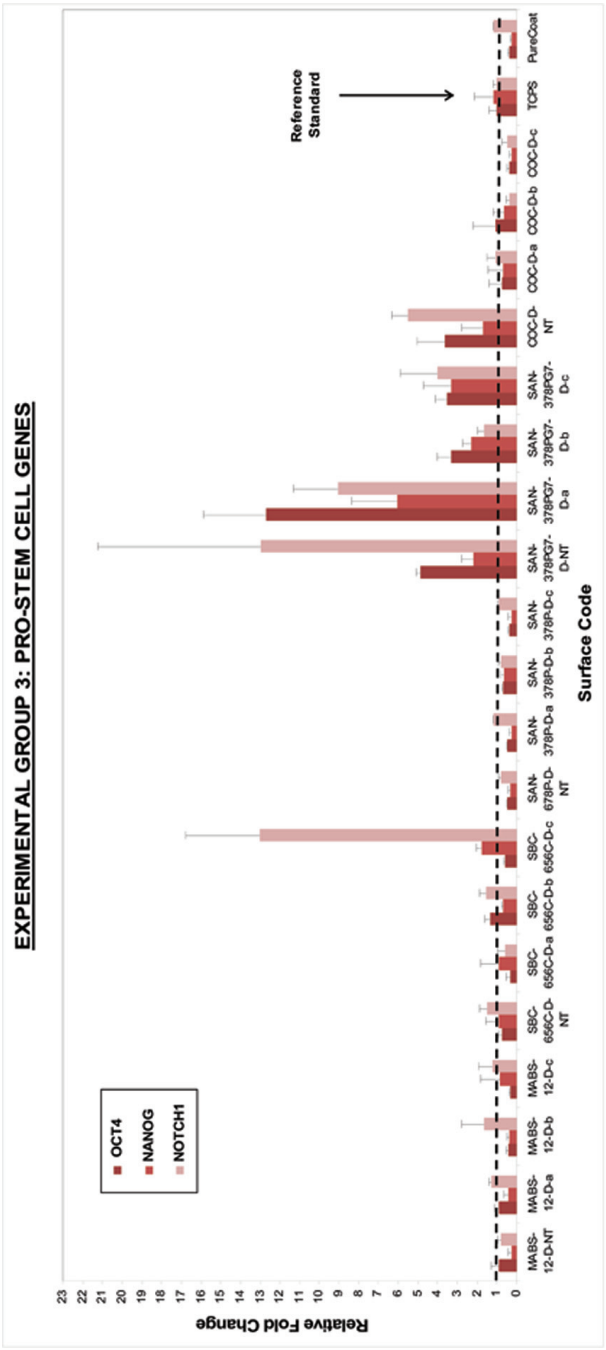
EXPERIMENTAL GROUP 3: PRO-STEM CELL GENES
OCT4
NANOG
NOTCH1
Relative Fold Change
Surface Code
Reference Standard
MABS-12-D-NT
MABS-12-D-a
MABS-12-D-b
MABS-12-D-c
SBC-656C-D-NT
SBC-656C-D-a
SBC-656C-D-b
SBC-656C-D-c
SAN-678P-D-NT
SAN-378P-D-a
SAN-378P-D-b
SAN-378P-D-c
SAN-378PG7-D-NT
SAN-378PG7-D-a
SAN-378PG7-D-b
SAN-378PG7-D-c
COC-D-NT
COC-D-a
COC-D-b
COC-D-c
TCPS
PureCoat

(a)

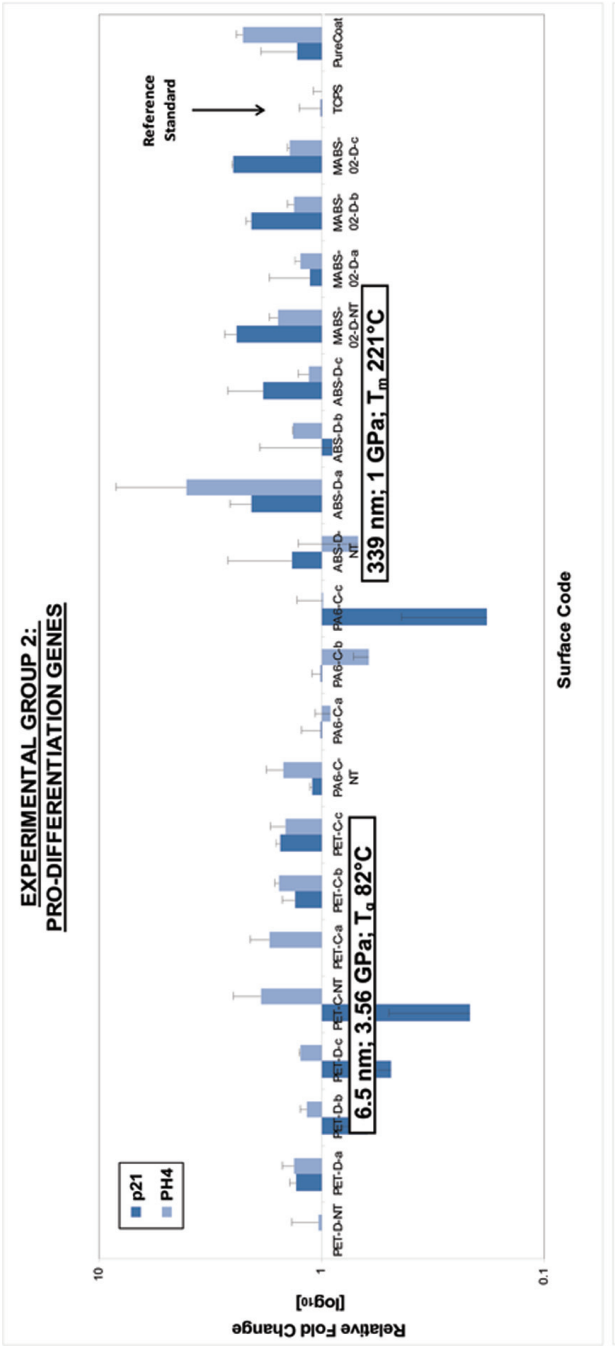
EXPERIMENTAL GROUP 2:
PRO-DIFFERENTIATION GENES
p21
PH4
Relative Fold Change
[log10]
10
1
0.1
Reference Standard
6.5 nm; 3.56 GPa; Ta 82°C
339 nm; 1 GPa; Tm 221°C
PET-D-NT
PET-D-a
PET-D-b
PET-D-c
PET-C-NT
PET-C-a
PET-C-b
PET-C-c
PA6-C-NT
PA6-C-a
PA6-C-b
PA6-C-c
ABS-D-NT
ABS-D-a
ABS-D-b
ABS-D-c
MABS-02-D-NT
MABS-02-D-a
MABS-02-D-b
MABS-02-D-c
TCPS
PureCoat
Surface Code

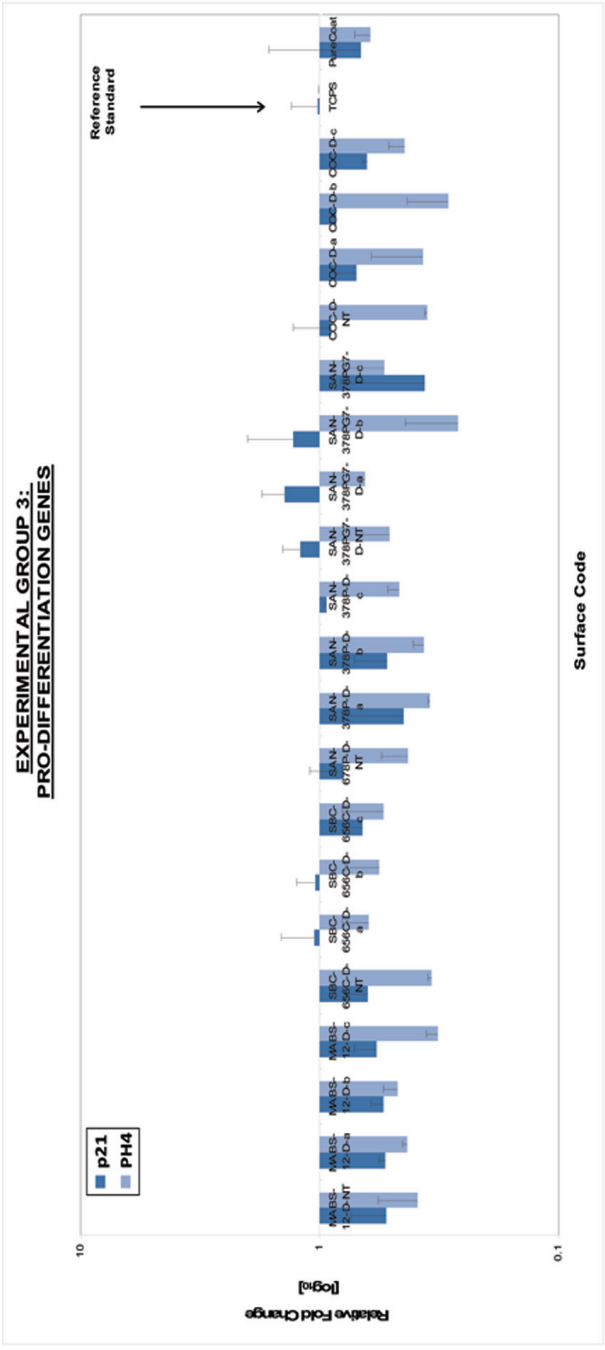

(b)

Figure 6.4 Effects of additional plastic surfaces on relative pro-stem cell and pro-differentiation gene expression in MSC cultures. Experiments were performed as in *Figure 6.3* but with additional surfaces examining the effects on gene expression related to (a) MSC maintenance (OCT4, NOTCH1, NANOG) or (b) differentiation (p21, PH4). Normalizations were performed with β-actin, and values were arbitrarily assigned a value of 1 relative to BD TCPS Falcon. BD PureCoat Amine plates also served as a reference material.

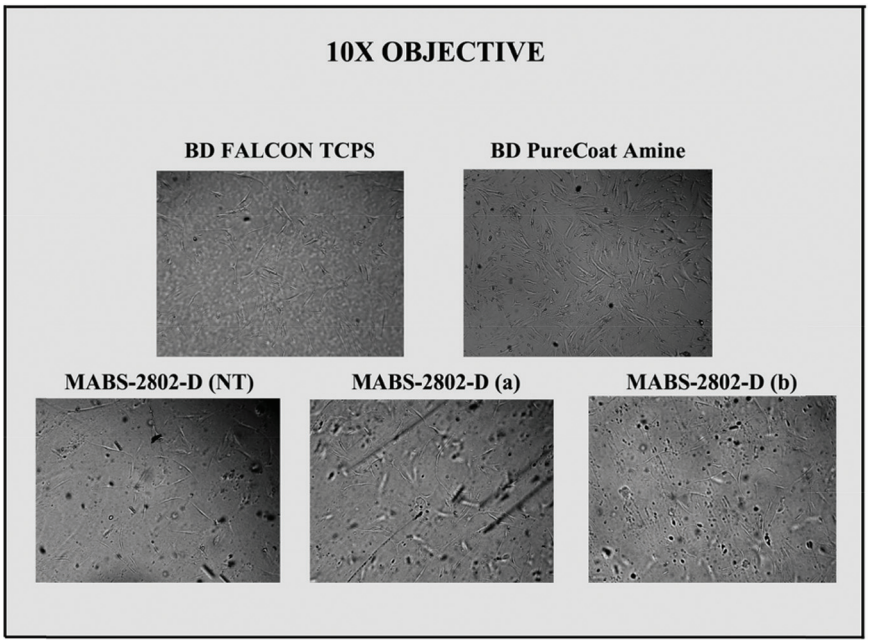

Figure 6.5 Representative pictographs of hMSC grown on control and test surfaces for 5 days. Images from cells grown on several non-opaque surfaces were included to show morphology on test coverslips.

currently the best available surface for expanding MSC. However, the use of TCPS is limited by changes in cell growth and function with extended culturing. Clinical applications require consistencies amongst the stem cells for extended periods of time. Part of the inconsistencies observed within labs culturing stem cells on these surfaces, may be due to the aging of the plasma-treated plates. Herein we studied the growth of hMSCs on several plastic surfaces in order to identify materials which outperform conventional TCPS, and that can potentially facilitate stem cell differentiation into specialized tissues.

Plasmas are often used to alter the surface properties of polymers and insert chemically reactive functionalities. The plasma discharge causes molecular fragmentations, bond fissions and ionizations generating reactive species and high energy photons that engage in subsequent reactions, resulting in cleaning, ablation, crosslinking, and surface chemical functionalization of the plasma-treated substrates. Typically noble gas plasmas (e.g., He or Ar) are

effective in etching the surface whereas chemically reactive plasmas add new functional groups. The significant decrease in contact angle of our plasma treated coverslips is indicative of increased surface hydrophilicity. Under the experimental conditions used, the depth of plasma surface modification is about 20 Å. Select coverslip surfaces were analyzed by XPS to determine the elemental surface composition and extent of surface derivatization. Since the XPS depth of analysis is 100 Å, the data reported in Table 6.3 averages the elemental analysis of the derivatized surfaces with the bulk values. One limitation of XPS is that it cannot detect hydrogen, therefore the ratio of elements reported discounts the presence of hydrogen.

The XPS spectra are obtained by irradiating the material to be analyzed with a beam of X-rays while simultaneously measuring the kinetic energy and number of electrons that escape from the surface. The output data is the binding energy of the ejected electron which relates to the orbital from which the electron is ejected, characteristic of each element. The number of electrons detected with a specific binding energy is proportional to the number of corresponding atoms in the sample. This then provides the percent of each atom in the sample. The chemical environment and oxidation state of the atom can be determined through the shifts of the peaks within the range expected. If the electrons are shielded then it is easier, or requires less energy, to remove them from the atom, i.e., the binding energy is low. The corresponding peaks will shift to a lower energy in the expected range. If the core electrons are not shielded as much, such as the atom being in a high oxidation state, then just the opposite occurs.

With the exception of POM, all other plasma treatments enhanced the oxygen content of the plastics therefore oxidizing the surface by incorporation of oxygen-containing moieties (O/C ratio increases after treatment). For example, the XPS data of the coverslips made from SBC 656 C showed not only an increase of the elemental oxygen percentage at the surface after plasma treatment, but also an increase of the fraction of carbon atoms with higher oxidation state. The aliphatic hydrocarbon sp^3 carbon (1s) binding energy is 284.8 eV. Electronegative substituents decrease the electron density on the carbon atom causing small increases in the C(1s) binding energies. The experimental C(1s) spectra for SBC 656 C were resolved by including Gaussian contributions from higher binding energy peaks normally assigned to C(1s) substituted with oxygen. The nitrogen enrichment at the surface was the highest for plasma treatment (a), employing a gaseous mixture of ammonia and hydrogen. The binding energy of the N(1s) peak at 399 eV corresponds to

sp^3 nitrogen bonded to sp^3 hybridized carbon, and is good evidence for amine groups on the surface [28, 29]. The chemical state identifications based on the measured binding energies are presented in Table 6.4. The fitting of the XPS peaks is presented in Figure 6.6.

Plasma treatment suffers from a short-lived nature as treated chains could reptate into the polymer bulk with the surface reverting partly to the original untreated state. This may lead to significant variability as the surface chemical composition changes upon storage after plasma fabrication. The plasma conditions used herein are known to generate chemically-modified surfaces stable for at least 2 months. However, two months after plasma treatment all surfaces had their contact angle reversed to almost the initial values before treatment. Surface aging seems to depend on the polymer chain flexibility (T_g) and should be taken into account as they could contribute to product variability.

The coverslips made with molds having a matte finish had high roughness (RMS 167–434 nm). The coverslips made with molds having a glossy finish had very low surface roughness (RMS 6–18 nm), with the exception of SAN 378 PG-7 (RMS 235nm) (Figure 6.7). This plastic is a tough glass fiber-reinforced SAN (30% glass fiber) with the highest modulus in the series of 12 GPa.

All test surfaces were divided into three experimental groups which were analyzed independently. BD TCPS Falcon and BD PureCoat Amine plates served as reference standards. The effects of the BASF polymeric surfaces on stem cell maintenance and differentiation were screened by stem cell specific (OCT-4; NOTCH1; FOXD3) and differentiation specific (PH-4; p63) biomarkers. In analyzing the data, an increase in the stem cell specific or a decrease in the differentiation-specific genes indicates a "positive result" compared to reference standard. For the first experimental group, "positive results" in two of the three studied genes was viewed as warranting further analysis. For the second and third experimental groups, "positive results" in three of the five studied genes was viewed as warranting further analysis.

The following plastic surfaces represent positive hints: (a) in experimental group 1 surfaces POM G-a, POM G-b, and POM M1-c with better than reference standard in 2 of 3 stem cell-specific genes; (b) in experimental group 2 surfaces PA6 M1-a, PA6 M1-b, and ABS G-NT with 3 of 5 stem cell- or differentiation-specific genes better then reference; and (c) in experimental group 3 surfaces SBC 656 C G-c, SAN 378 PG-7 G-NT, SAN 378 PG-7 G-a, SAN-378PG7 G-b, and COC G-NT with 4 of 5 genes better than

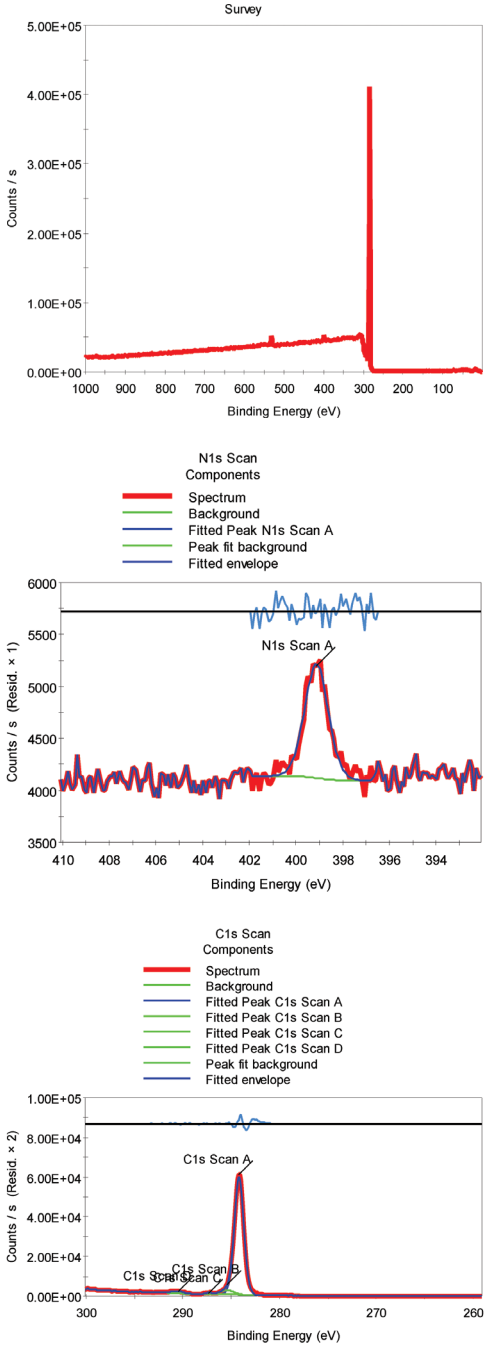
Survey
5.00E+05
4.00E+05
3.00E+05
2.00E+05
1.00E+05
0.00E+00
Counts / s
1000 900 800 700 600 500 400 300 200 100
Binding Energy (eV)
N1s Scan
Components
Spectrum
Background
Fitted Peak N1s Scan A
Peak fit background
Fitted envelope
6000
5500
5000
4500
4000
3500
Counts / s (Resid. × 1)
N1s Scan A
410 408 406 404 402 400 398 396 394
Binding Energy (eV)
C1s Scan
Components
Spectrum
Background
Fitted Peak C1s Scan A
Fitted Peak C1s Scan B
Fitted Peak C1s Scan C
Fitted Peak C1s Scan D
Peak fit background
Fitted envelope
1.00E+05
8.00E+04
6.00E+04
4.00E+04
2.00E+04
0.00E+00
Counts / s (Resid. × 2)
C1s Scan A
C1s Scan B
C1s Scan C
300 290 280 270 260
Binding Energy (eV)

(a)

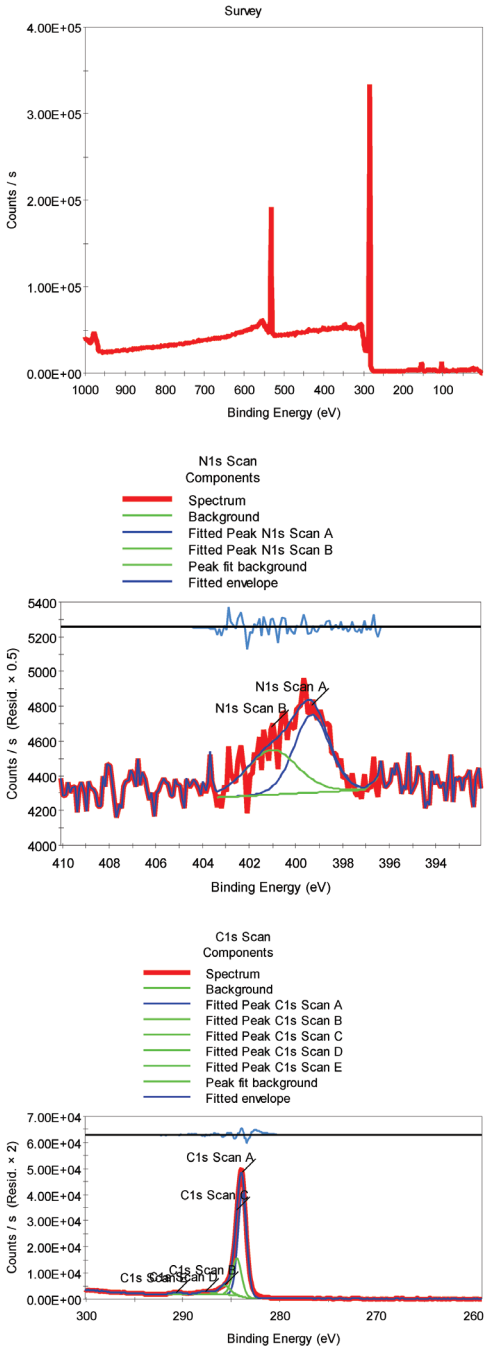
Survey
Counts / s
Binding Energy (eV)
N1s Scan
Components
Spectrum
Background
Fitted Peak N1s Scan A
Fitted Peak N1s Scan B
Peak fit background
Fitted envelope
N1s Scan A
N1s Scan B
Counts / s (Resid. × 0.5)
Binding Energy (eV)
C1s Scan
Components
Spectrum
Background
Fitted Peak C1s Scan A
Fitted Peak C1s Scan B
Fitted Peak C1s Scan C
Fitted Peak C1s Scan D
Fitted Peak C1s Scan E
Peak fit background
Fitted envelope
C1s Scan A
C1s Scan C
C1s Scan B
C1s Scan D
Counts / s (Resid. × 2)
Binding Energy (eV)

(b)

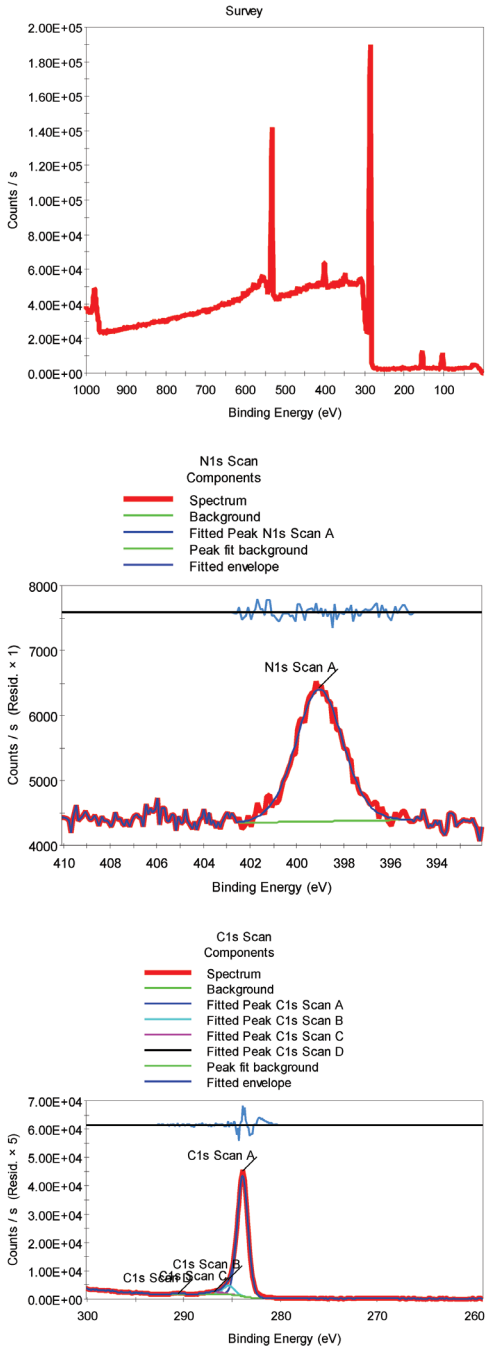
Survey
Counts / s
Binding Energy (eV)
N1s Scan
Components
Spectrum
Background
Fitted Peak N1s Scan A
Peak fit background
Fitted envelope
N1s Scan A
Counts / s (Resid. × 1)
Binding Energy (eV)
C1s Scan
Components
Spectrum
Background
Fitted Peak C1s Scan A
Fitted Peak C1s Scan B
Fitted Peak C1s Scan C
Fitted Peak C1s Scan D
Peak fit background
Fitted envelope
C1s Scan A
C1s Scan B
C1s Scan C
C1s Scan D
Counts / s (Resid. × 5)
Binding Energy (eV)

(c)

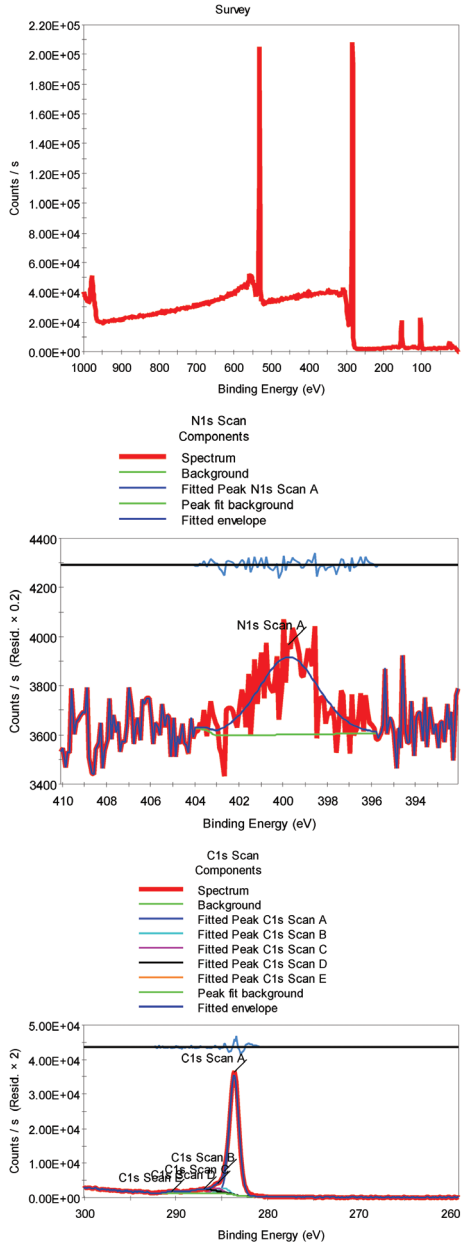

(d)

Figure 6.6 XPS spectra, C(1s), and N(1s) peak fittings of SBC 656 C coverslips: (a) SBC 656 C G-NT; (b) SBC 656 C G-a; (c) SBC 656 C G-b; and (d) SBC 656 C G-c. The peaks were fit with Gaussian line-shapes after background subtraction.

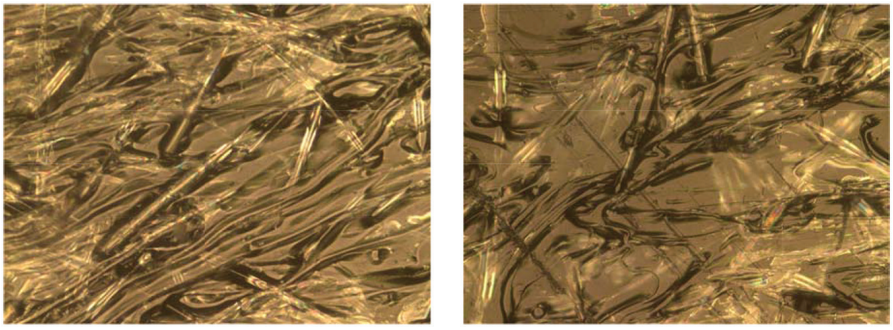

Figure 6.7 Optical micrograph pictures of SAN 378 PG-7 (G-c) coverslips. The pictures were taken with a Nikon Inverted Metallurgical Epiphot 200 in the darkfield reflective mode.

reference, and surface SAN 378 PG-7 G with 5 of 5 genes better than reference. Of the many surface physical characteristics the roughness and fibrous structure of the glass fiber-reinforced poly(styrene-acrylonitrile) SAN 378 PG-7 surface had the most prevalent effect on facilitating MSC expansion with preservation of stem cell function.

6.5 Conclusions

We tested a panel of plastic surfaces with different physical characteristics in order to identify materials which outperform conventional tissue culture polystyrene (TCPS) in their ability to expand and maintain hMSCs in an undifferentiated state. Several surfaces exhibited a statistically significant increase in the stem cell specific-genes and/or a decrease in the differentiation-specific genes, indicating a "positive result" compared to the TCPS reference standard. The plastics with positive results did not correlate with a specific surface chemistry or plasma treatment. Of the many surface physical characteristics, the roughness and fibrous structure of a glass fiber-reinforced poly(styrene-acrylonitrile) polymeric surface had the most prevalent effect on facilitating hMSC expansion with preservation of stem cell function. These findings highlight, in particular, the important role of the surface mechanical properties in cell/material interactions. Future investigations are planned to validate these results across multiple cell culture passages, involving the effects on cell phenotype, long-term morphology, protein expression, and functional assessment.

Acknowledgements

The authors would like to acknowledge Dr. Nancy Brungard and Melissa Thornton from BASF, Iselin, NJ, for performing the XPS experiments, and Dr. Rachel Dong and Corola Jernigan from BASF, Tarrytown, NY, for the AFM and optical microscope analysis.

References

[1] Yan, Y., et al., *Directed differentiation of dopaminergic neuronal subtypes from human embryonic stem cells.* Stem cells, 2005. **23**(6): 781–90.

[2] Kim, N.R., et al., *Discovery of a new and efficient small molecule for neuronal differentiation from mesenchymal stem cell.* Journal of medicinal chemistry, 2009. **52**(24): 7931–3.

[3] Totey, S. and R. Pal, *Adult stem cells: a clinical update.* Journal of stem cells, 2009. **4**(2): 105–21.

[4] Trzaska, K.A., et al., *Brain-derived neurotrophic factor facilitates maturation of mesenchymal stem cell-derived dopamine progenitors to functional neurons.* Journal of neurochemistry, 2009. **110**(3): 1058–69.

[5] Momin, E.N., et al., *Mesenchymal stem cells: new approaches for the treatment of neurological diseases.* Current stem cell research & therapy, 2010. **5**(4): 326–44.

[6] Patel, N., et al., *Developmental regulation of TAC1 in peptidergic-induced human mesenchymal stem cells: implication for spinal cord injury in zebrafish.* Stem cells and development, 2012. **21**(2): 308–20.

[7] Campagnoli, C., et al., *Identification of mesenchymal stem/progenitor cells in human first-trimester fetal blood, liver, and bone marrow.* Blood, 2001. **98**(8): 2396–402.

[8] Castillo, M., et al., *The immune properties of mesenchymal stem cells.* International journal of biomedical science: IJBS, 2007. **3**(2): 76–80.

[9] Dominici, M., et al., *Heterogeneity of multipotent mesenchymal stromal cells: from stromal cells to stem cells and vice versa.* Transplantation, 2009. **87**(9 Suppl): S36–42.

[10] Cho, K.J., et al., *Neurons derived from human mesenchymal stem cells show synaptic transmission and can be induced to produce the neurotransmitter substance P by interleukin-1 alpha.* Stem cells, 2005. **23**(3): 383–91.

[11] Greco, S.J., et al., *An interdisciplinary approach and characterization of neuronal cells transdifferentiated from human mesenchymal stem cells.* Stem cells and development, 2007. **16**(5): 811–26.

[12] Greco, S.J., et al., *Synergy between the RE-1 silencer of transcription and NFkappaB in the repression of the neurotransmitter gene TAC1 in human mesenchymal stem cells.* The Journal of biological chemistry, 2007. **282**(41): 30039–50.

[13] Cho, J., P. Rameshwar, and J. Sadoshima, *Distinct roles of glycogen synthase kinase (GSK)-3alpha and GSK-3beta in mediating cardiomyocyte differentiation in murine bone marrow-derived mesenchymal stem cells.* The Journal of biological chemistry, 2009. **284**(52): 36647–58.

[14] Potian, J.A., et al., *Veto-like activity of mesenchymal stem cells: functional discrimination between cellular responses to alloantigens and recall antigens.* Journal of immunology, 2003. **171**(7): 3426–34.

[15] Chan, J.L., et al., *Antigen-presenting property of mesenchymal stem cells occurs during a narrow window at low levels of interferon-gamma.* Blood, 2006. **107**(12): 4817–24.

[16] Romieu-Mourez, R., et al., *Regulation of MHC class II expression and antigen processing in murine and human mesenchymal stromal cells by IFN-gamma, TGF-beta, and cell density.* Journal of immunology, 2007. **179**(3): 1549–58.

[17] Le Blanc, K., et al., *Mesenchymal stem cells for treatment of steroid-resistant, severe, acute graft-versus-host disease: a phase II study.* Lancet, 2008. **371**(9624): 1579–86.

[18] Stagg, J., *Immune regulation by mesenchymal stem cells: two sides to the coin.* Tissue antigens, 2007. **69**(1): 1–9.

[19] Greco, S.J. and P. Rameshwar, *Microenvironmental considerations in the application of human mesenchymal stem cells in regenerative therapies.* Biologics: targets & therapy, 2008. **2**(4): 699–705.

[20] Buron, F., et al., *Human mesenchymal stem cells and immunosuppressive drug interactions in allogeneic responses: an in vitro study using human cells.* Transplantation proceedings, 2009. **41**(8): 3347–52.

[21] Wang, Y., et al., *Bone marrow-derived mesenchymal stem cells inhibit acute rejection of rat liver allografts in association with regulatory T-cell expansion.* Transplantation proceedings, 2009. **41**(10): 4352–6.

[22] Tao, X.R., et al., *Clonal mesenchymal stem cells derived from human bone marrow can differentiate into hepatocyte-like cells in injured livers of SCID mice.* Journal of cellular biochemistry, 2009. **108**(3): 693–704.

[23] Mohseny, A.B., et al., *Osteosarcoma originates from mesenchymal stem cells in consequence of aneuploidization and genomic loss of Cdkn2.* The Journal of pathology, 2009. **219**(3): 294–305.

[24] Molcanyi, M., et al., *Developmental potential of the murine embryonic stem cells transplanted into the healthy rat brain–novel insights into tumorigenesis.* Cellular physiology and biochemistry: international journal of experimental cellular physiology, biochemistry, and pharmacology, 2009. **24**(1–2): 87–94.

[25] Shyong Siow, K., et al., *Plasma methods for the generation of chemically reactive surfaces for biomolecule immobilization and cell colonization – A review.* Plasma processes and polymers, 2006. **3**: 392–418.

[26] Hartwig, A. et al., *Smolders surface amination of poly(acrylonitrile).* Advances in colloid and interface science, 1994. **52**: 5–78.

[27] Klages, C.P., et al., *Atmospheric-pressure plasma amination of polymer surfaces*. Journal of adhesion science and technology, 2010. **24**: 1167–1180.

[28] Gammona, W.J., et al., *Experimental comparison of N(1s) X-ray photoelectron spectroscopy binding energies of hard and elastic amorphous carbon nitride films with reference organic compounds*. Carbon, 2003. **41**: 1917–1923.

[29] Nagatsu, M., et al., *Functionalization of polymer surfaces using microwave plasma chemical modification*. Journal of photopolymer science and technology, 2008. **21**(2): 257–261.